Since January 2020 Elsevier has created a COVID-19 resource centre with free information in English and Mandarin on the novel coronavirus COVID-19. The COVID-19 resource centre is hosted on Elsevier Connect, the company's public news and information website.

Journal of Molecular Liquids 337 (2021) 116440

Contents lists available at ScienceDirect

Journal of Molecular Liquids

journal homepage: www.elsevier.com/locate/molliq

Inhibition of SARS-CoV-2 reproduction using Boswellia carterii: A theoretical study

Mustafa M. Kadhim [a,*], Abbas Washeel Salman [b], Ameerah Mrebee Zarzoor [c], Wesam R. Kadhum [d]

[a] Department of Dentistry, Kut University College, Kut, Wasit 52001, Iraq
[b] Department of Production, College of Agriculture, Wasit University, Kut, Wasit 52001, Iraq
[c] Middle Technical University, Baghdad, Iraq
[d] Department of Pharmacy, Kut University College, Kut, Wasit 52001, Iraq

ARTICLE INFO

Article history:
Received 17 March 2021
Revised 30 April 2021
Accepted 5 May 2021
Available online 8 May 2021

Keywords:
SARS-CoV-2
COVID-19
Boswellia carterii
Autodock
DFT
MEP

ABSTRACT

This study investigated the possibility of inhibition of the SARS-CoV-2 virus using the compounds alpha-Boswellic acid (ABA) and beta-Boswellic acid (BBA) which are active components in the well-known natural product Boswellia carterii (BC). The SARS-CoV-2 virus reproduces in the body by linking its spike with the cell receptor. At the same time, a pH range (4.5–6) of the cell's lysosomes is considered as a perfect environment to release RNA in the cell cytoplasm. In view of these, docking studies were employed to study the interaction between the spikes of the virus and ABA or BBA using Molecular Graphic Laboratory (MGL) tools and AutoDock Vina application. The binding of the ABA and BBA with the spike of the virus could inhibit its reproduction or provide sufficient time for the immune system to recognize the virus and hence, produce suitable antibodies. In addition, the pKa of ABA, BBA and hydroxychloroquine (HCQ) were calculated using HF/6-311G (d,p) method and then they were compared with the experimental pKa of HCQ. The Lethal Concentrations (LC50) of ABA and BBA were also calculated. In addition, molecular electrostatic potential is reported which indicates the active sites of ABA and BBA.

1. Introduction

Coronaviruses are a large group of single-strand RNA viruses [1]. Recently COVID-19 pandemic appeared in Wuhan, China [2] and became a global concern in a very short period. To date, more than 100 million individuals were infected and more than 2 million were killed with a mortality rate of about 2.17% based on the World Health Organization. The ability of the virus leading to human–human infections raises lots of attention and is a major concern. International air travel and sometime, the lack of awareness have played a key role in the transmission of the virus. Recently, the complete genome sequence of the virus was listed in the National Center for Biotechnology Information (GenBank: MN908947.3). This helped in the determination of the structure and glycosylation pattern of the viral proteins and the method of interaction with the host cell. Like the other coronaviruses, the outer membrane has a spike glycoprotein responsible for its glycosylation [3]. It is reported that chloroquine (CQ) phosphate, inhibits COVID-19 infection in vitro [4]. CQ (N4-(7-Chloro-4-quinolinyl)-N 1,N1-diethyl-1,4- pentane diamine) has been used against amebiasis and malaria, but the uses of this drug were limited for several reasons; one of them is the overdose of CQ could cause acute poisoning and death, and the other is that it can lead to eye damage, heart disease, worsen skin conditions and it is fatal for some children [5]. Thus, there has been increasing interest in the derivatives of CQ. For instance, hydroxychloroquine (HCQ) sulfate, was prepared in 1946 by introducing a hydroxyl group into CQ and it was found to be less toxic than CQ in animals [6]. HCQ is a weak base, it elevates the pH of acidic intracellular organelles such as lysosomes, which is important for the fusion of membrane [7]. Recent studies [8,9] indicate that HCQ blocks the transport of COVID-19 from early to late endosomes, which appears to be a requirement to release the viral genome as in the case of SARS-CoV [10,11]. Theoretical calculations, particularly density functional theory (DFT) method has been used to predict the most stable conformation for different compounds and isomers [12–14]. Further, it is used in combination with docking, which helps to rationalize the design of new therapeutic agents for treating the human disease [15,16].

This research work proposes a method to inhibit virus activity complications and even give the infected body enough time to produce suitable antibodies. Docking and DFT computations were used to estimate the interaction of the natural products ABA and

* Corresponding author.
E-mail address: Mustafa.mohammed@alkutcollege.edu.iq (M.M. Kadhim).

https://doi.org/10.1016/j.molliq.2021.116440
0167-7322/

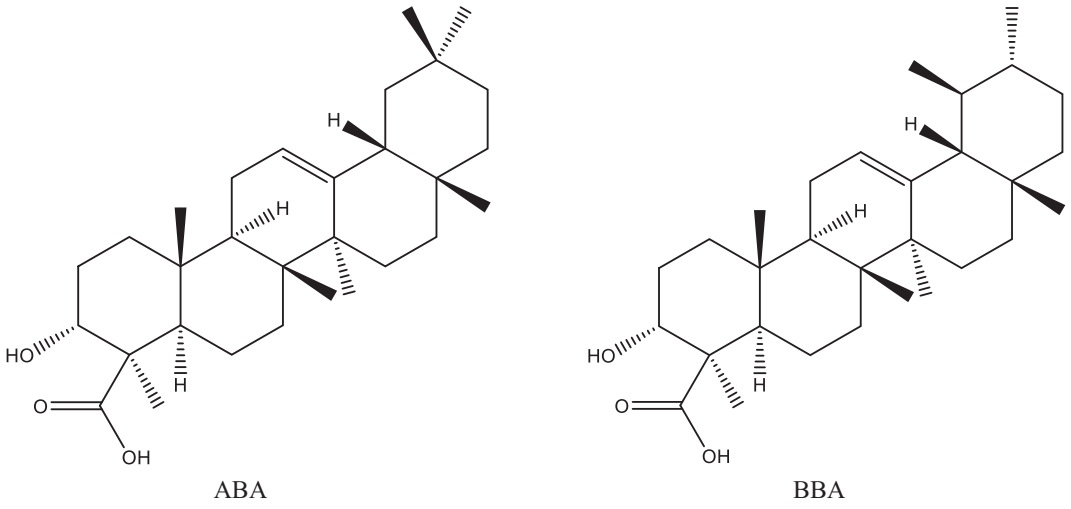

Fig. 1. Structures of ABA and BBA.

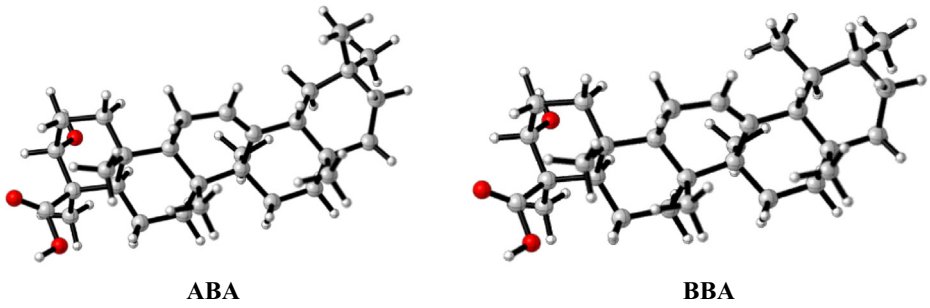

Fig. 2. Optimized structures of ABA and BBA using the B3LYP/6-311G(d,p) method.

BBA (Fig. 1), which is used to treat indigestion with the viral glycoprotein in the spike. ABA and BBA were chosen based on their biological activity in previous studies [9,17,18] and it is known to have minimum side effect according to BC products [19]. We also compared ABA and BBA with HCQ as a standard antiviral drug to determine whether they would give the same effect as for the HCQ or not.

2. Computational methods

The protein structure downloaded by (Research Collaboratory for Structural Bioinformatics) RCSB [15] using Molecular Graphic Laboratory (MGL) tools and AutoDock Vina application [16,17]. The coordinates of the spike structure and the ligands (ABA and BBA) were separated with the help of Autodock tools (ADT, version 1.5.6). The SARS-CoV-2 spike glycoprotein-S1 protein and ligands structures were processed to a format recognized by the ADT (*. pdbqt files) by adding all hydrogen atoms, Gasteiger charges, and merging the polar hydrogen atoms. The Autodock often tries to identify the root for the molecule unless the user specifies it. In this work, the Autodock automatically selected the root. The atoms specific affinity maps for all ligand atom types, electrostatic and desolation potentials were computed with the help of Auto grid (version 4.2.6) [18]. PyMol was used to analyze the results [19–24]. ABA and BBA were optimized in the gas phase, without any symmetry restriction, before the docking process using Gaussian 16 [25] based on the DFT method with the B3LYP functional [26,27] in conjunction with the 6–311++G(d) basis set [28]. The optimization was followed by frequency computations to ensure that the complex was a true local minimum. The optimized structures of ABA and BBA are illustrated in Fig. 2 and their coordinates are provided in **Table SI1** (supplementary information). The molecular electrostatic potential (MEP) was also investigated by using unrestricted DFT method and 6-31G (d,p) basis set.

3. Results and discussion

3.1. Spike-ABA and -BBA interactions

The active functional groups in ABA and BBA are OH and COOH and according to geometry optimization, there are planarities in some parts (according to cis and trans of atoms in the molecules, each four atom of cis are near to zero and trans near to 180°). On the basis of MEP (Fig. 3), there is high electron density (red color) on the regions involving the OH and COOH groups [22]. The structure code from PDB is (6acd) Fig. 4. We compared the best sites to link with the protein by calculating the binding energy [29]. The range of binding energy values are −7.3 to −8.0 kcal/mol for ABA and −7.2 to −7.7 kcal/mol for BBA. The better location of the bonded protein turns out at (-7.7 kcal/mol) for both with ABA and BBA. The bond lengths of the interacted OH and COOH are 3.0 and 3.1 Å respectively (Fig. 5**)**. In addition, protein-BBA$_{(OH)}$ bond length is 3.22 Å. The analysis of the results using DSV program shows the interaction between the amino acid consistence spike and ABA (Fig. 6**)**. There is hydrogen bonding between the carboxyl group and ARG, while van der Waals forces with SER. Further, all hydrogen atoms could interacts with protein. In BBA, there is van der Waals interaction between the terminal alkyl ring and the LYS, while there is a chemical interaction between LEU with the carboxyl group. These results support the link between

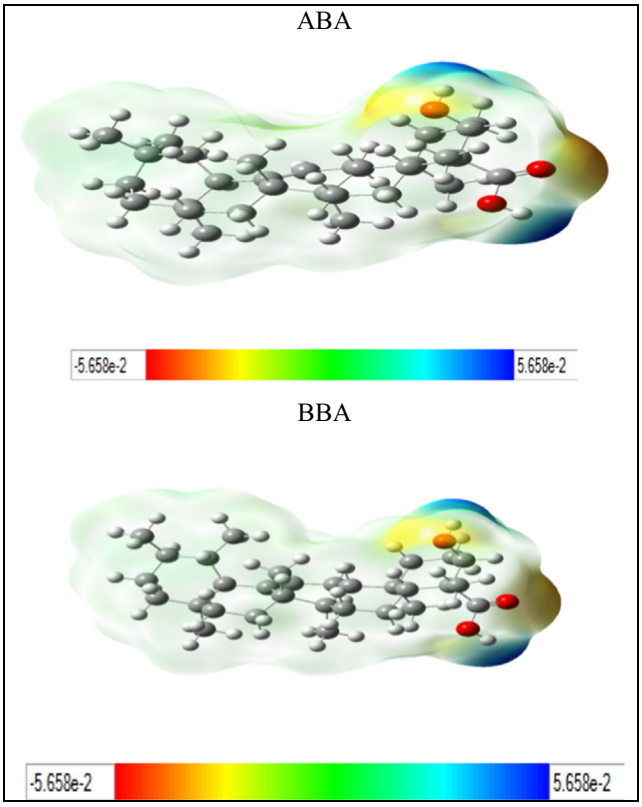

Fig. 3. MEP surfaces of ABA and BBA.

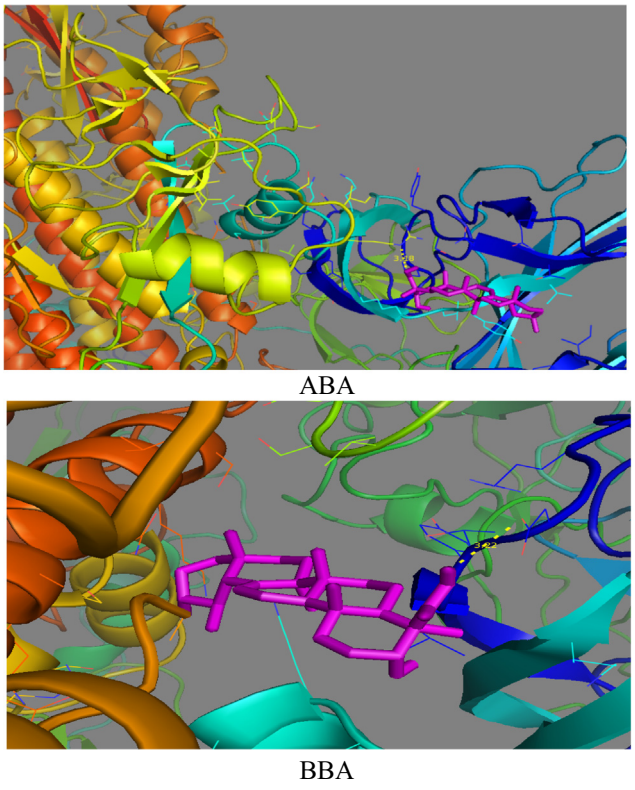

Fig. 5. ABA and BBA compounds with spike protein linkage.

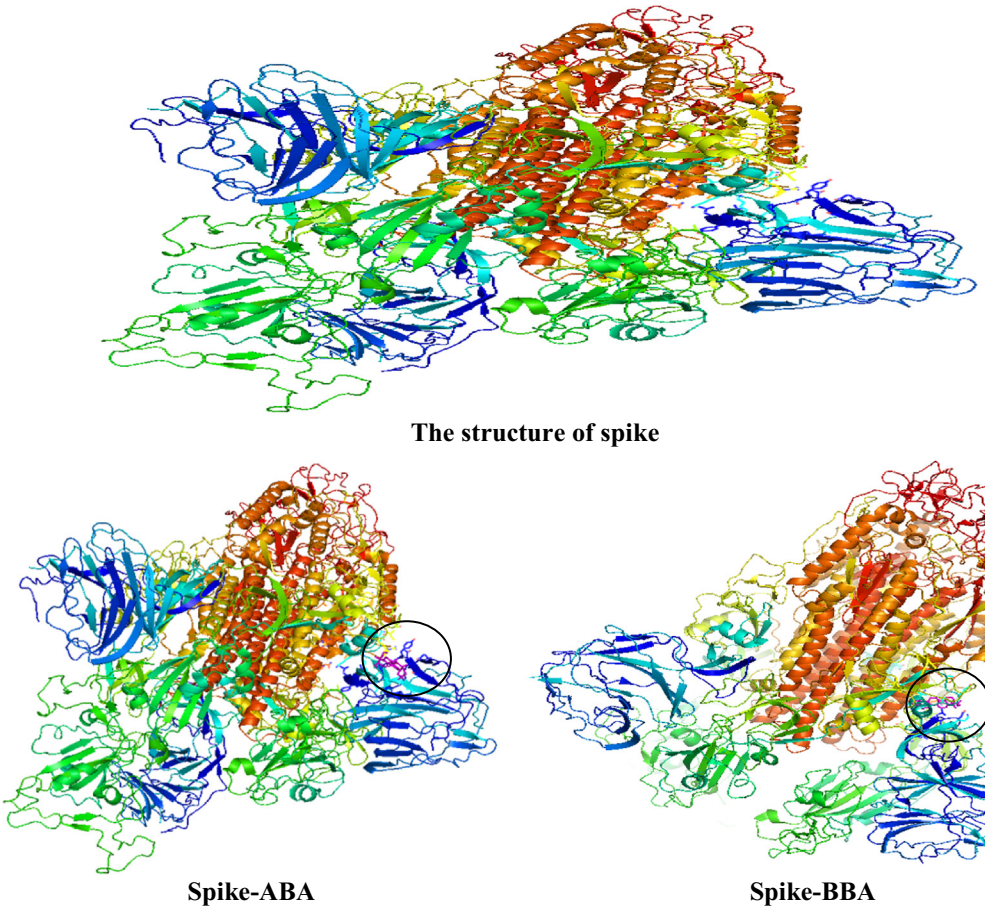

Fig. 4. The interaction of ABA and BBA with protein of spike parts.

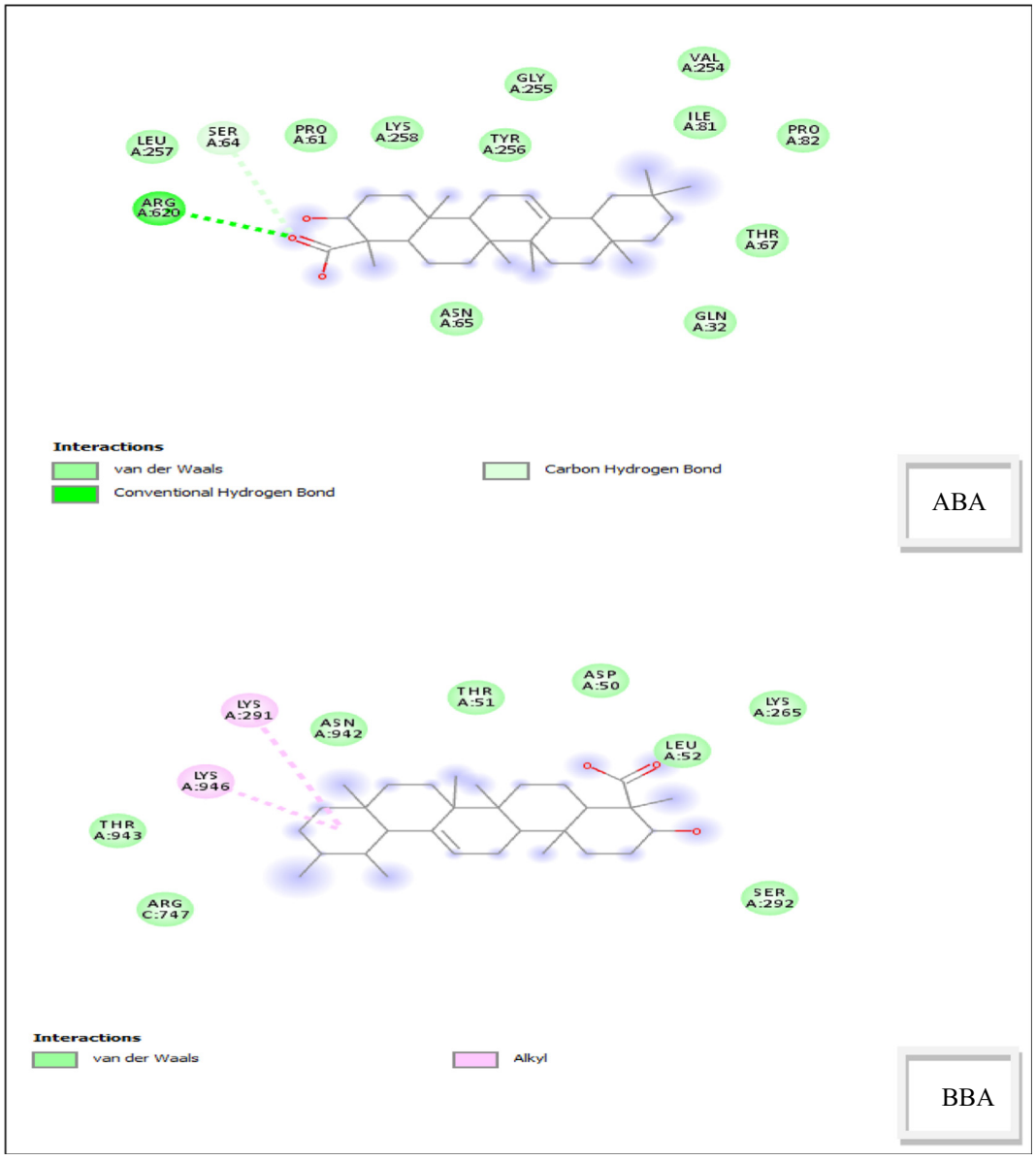

Fig. 6. Two dimension interactions structures of ABA and BBA.

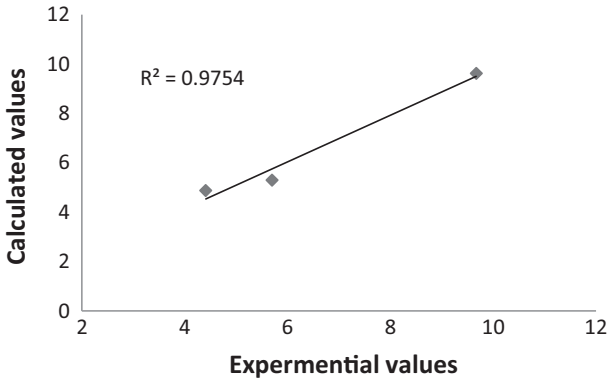

Fig. 7. Plot of the experimental versus theoretical values of pKa for ABA, BBA and HCQ.

the protein and the inhibitor. On this basis, blocking the spike of the virus can delay its adhesion to the surface of the cell. Therefore, this process could provide additional time for the body to prepare an environment for antibodies.

3.2. ABA and BBA activity

A previous study proved the different pH in the range of (4.5–6) that could prevent virus reproduction by inhibiting the glycosylation enzymes which in turn release the RNA in cell cytoplasm [8,30]. From these studies, the pKa of the compounds used to confirm the calculations, and the regression correlation coefficient (R^2) values is 0.9754 (Fig. 7). Gibbs free energy was calculated by HF/frequently (6-311G++/p,d) basis set. Equation (1) was used to estimate the pKa of HCQ, ABA and BBA compounds at 298 K [31,32].

$$pKa = (\Delta G_{sol}/1.364) - \log [H_2O] \quad (1)$$

Where the ΔG_{sol} is a Gibbs free energy and was calculated by **Equations (2) and (3)**, $[H_2O]$ is the water concentration.

$$\Delta G_{sol} = \Delta G_g + \Delta G_{sol}(A^-) + \Delta G_{sol}(H_3O^+) - \Delta G_{sol}(HA) - \Delta G_{sol}(H_2O) \quad (2)$$

$$\Delta G_{sol} = \Delta G_g + \Delta G_{sol}(HA^+) + \Delta G_{sol}(OH^-) - \Delta G_{sol}(HA) - \Delta G_{sol}(H_2O) \quad (3)$$

All parameters for ABA and BBA were calculated according to the cycle:

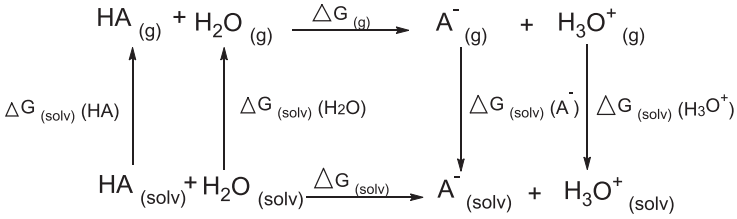

While the HCQ parameters calculated by the cycle:

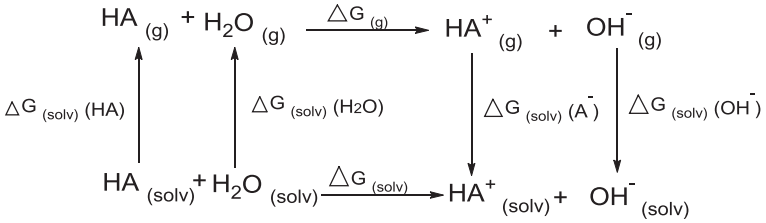

The ΔG_{solv} values of ABA, BBA and HCQ are 15.64, 14.97 and 21.36 kcal/mol, respectively (Table 1). The reported value of pKa for HCQ is 9.67, which differs with the theoretical by 0.06 [33]. The calculated pKa of ABA and BBA compounds found to be 5.30 and 4.88, respectively, while the experimental values are 5.70 and 4.41 [34,35]. The acidity order of the compounds studied is BBA > ABA > HCQ. The values indicate the acidity of ABA, BBA and the basicity of HCQ.

3.3. Lethal concentration method (LC50)

LC50 is the maximum concentration nontoxic per Kilogram and **Equation 4** used to estimate the LC50 values.

$\text{Log LC50} = 38.00 - 1.13 \times S_{tr} + 1.38 \times 10^{-3} \times \omega H - 2.22 \times 10^{-3} \times \omega L - 0.36 \times I_A$ Equation 4

Where S_{tr} = Translational entropy, ω = vibrational wavenumber, I_A = principal moment of inertia, ωH = High frequency and ωL = Low frequency [36]. The LC50 values for ABA and BBA were 6.59×10^{-8} and 6.51×10^{-8} mol/L, respectively (Table 2). The results indicate that high concentration can be use in the human body for ABA and BBA.

Table 1
Parameters of thermodynamic calculations by HF method with experimental values.

Comp.	ΔG_g (kcal/mol)	ΔG_{sol} (kcal/mol)	pKa (Cal.)	pKa (Exp.)
HCQ	506.2	21.36	9.62	9.67
ABA	153.8	15.64	5.30	5.70
BBA	153.5	14.97	4.88	4.41

Table 2
Predicted toxicity parameters of the studied compounds (ABA and BBA).

Compound.	S_{tr}	I_A	ωH	ωL	LC50 (mol/L)
ABA	44.243	1	3792.41	26.88	6.59×10^{-8}
BBA	44.243	1	3792.34	29.33	6.51×10^{-8}

4. Conclusions

A theoretical study on ABA and BBA compounds as an active component from natural product Boswellia carterii to inhibit SARS-Cov-2 virus was carried out. Computational methods were used to study their binding to the spikes of the virus. The MEP showed that the ABA and BBA interaction sites are the OH and COOH groups. The binding energy indicates the high affinity between the spike proteins with the studied compounds. The calculations indicate hydrogen bonding and van der Waals forces for ABA and BBA interacting with the spikes. Hydroxychloroquine was compared with ABA and BBA using the calculated pKa values. The LC50 values indicated that a high amount of ABA and BBA could be used safely in the human body.

CRediT authorship contribution statement

Mustafa M. Kadhim: Project administration, Software, Methodology. **Abbas Washeel Salman:** Supervision, Investigation. **Ameera Mrebee Zarzoor:** Formal analysis, Resources. **Wesam R. Kadhum:** Formal analysis, Validation, Data curation.

Declaration of Competing Interest

The authors declare that they have no known competing financial interests or personal relationships that could have appeared to influence the work reported in this paper.

Acknowledgements

The authors acknowledge the facilities from their Universities.

References

[1] N. Decaro, A. Lorusso, Novel human coronavirus (SARS-CoV-2): A lesson from animal coronaviruses, Vet. Microbiol. 244 (2020) 108693, https://doi.org/10.1016/j.vetmic.2020.108693.

[2] C. Huang, Y. Wang, X. Li, L. Ren, J. Zhao, Y. Hu, L. Zhang, G. Fan, J. Xu, X. Gu, Z. Cheng, T. Yu, J. Xia, Y. Wei, W. Wu, X. Xie, W. Yin, H. Li, M. Liu, Y. Xiao, H. Gao, L. Guo, J. Xie, G. Wang, R. Jiang, Z. Gao, Q. Jin, J. Wang, B. Cao, Clinical features of patients infected with 2019 novel coronavirus in Wuhan, China, Lancet. 395 (2020) 497–506. https://doi.org/10.1016/S0140-6736(20)30183-5.

[3] S. Glycoprotein, F. Enteric, crossm Glycan Shield and Fusion Activation of a, Deltacoronavirus 92 (2018) 1–16.

[4] Z. He, B. Wang, C. Hu, J. Zhao, An overview of hydrogel-based intra-articular drug delivery for the treatment of osteoarthritis, Colloids Surfaces B Biointerfaces. 154 (2017) 33–39, https://doi.org/10.1016/j.colsurfb.2017.03.003.

[5] A. Iris, Review of side effects and toxicity of chloroquine / by H . Weniger Related items, (2020) 2020.

[6] Evan W. McChesney, Animal toxicity and pharmacokinetics of hydroxychloroquine sulfate, Am. J. Med. 75 (1) (1983) 11–18, https://doi.org/10.1016/0002-9343(83)91265-2.

[7] Mario Mauthe, Idil Orhon, Cecilia Rocchi, Xingdong Zhou, Morten Luhr, Kerst-Jan Hijlkema, Robert P. Coppes, Nikolai Engedal, Muriel Mari, Fulvio Reggiori, Chloroquine inhibits autophagic flux by decreasing autophagosome-lysosome fusion, Autophagy. 14 (8) (2018) 1435–1455, https://doi.org/10.1080/15548627.2018.1474314.

[8] Manli Wang, Ruiyuan Cao, Leike Zhang, Xinglou Yang, Jia Liu, Mingyue Xu, Zhengli Shi, Zhihong Hu, Wu Zhong, Gengfu Xiao, Remdesivir and chloroquine effectively inhibit the recently emerged novel coronavirus (2019-nCoV) in vitro, Cell Res. 30 (3) (2020) 269–271, https://doi.org/10.1038/s41422-020-0282-0.

[9] J. Liu, R. Cao, M. Xu, X. Wang, H. Zhang, H. Hu, Y. Li, Z. Hu, W. Zhong, M. Wang, Hydroxychloroquine, a less toxic derivative of chloroquine, is effective in inhibiting SARS-CoV-2 infection in vitro, Cell Discov. 6 (2020) 16, https://doi.org/10.1038/s41421-020-0156-0.

[10] C. Das, P. Sharma, K. Sinha, K. Rajarshi, Biophysical Chemistry Recent trends in analytical and digital techniques for the detection of the, Biophys. Chem. 270 (2021), https://doi.org/10.1016/j.bpc.2020.106538 106538.

[11] Rebecca M. Mingo, James A. Simmons, Charles J. Shoemaker, Elizabeth A. Nelson, Kathryn L. Schornberg, Ryan S. D'Souza, James E. Casanova, Judith M. White, R.W. Doms, Ebola Virus and Severe Acute Respiratory Syndrome Coronavirus Display Late Cell Entry Kinetics: Evidence that Transport to NPC1 + Endolysosomes Is a Rate-Defining Step, J. Virol. 89 (5) (2015) 2931–2943, https://doi.org/10.1128/JVI.03398-14.

[12] A.W. Salman, G.U. Rehman, N. Abdullah, S. Budagumpi, S. Endud, H.H. Abdallah, Synthesis, characterization, density function theory and catalytic performances of palladium(II)-N-heterocyclic carbene complexes derived from benzimidazol-2-ylidenes, Inorganica Chim. Acta. 438 (2015) 14–22, https://doi.org/10.1016/j.ica.2015.08.027.

[13] A.W. Salman, G. Ur Rehman, N. Abdullah, S. Budagumpi, S. Endud, H. Hadi Abdallah, W.Y. Wong, Sterically modulated palladium(II)-N-heterocyclic carbene complexes for the catalytic oxidation of olefins: Synthesis, crystal structure, characterization and DFT studies, Polyhedron. 81 (2014) 499–510, https://doi.org/10.1016/j.poly.2014.06.054.

[14] Abbas W. Salman, Rosenani A. Haque, Mustafa M. Kadhim, Frederick P. Malan, Ponnadurai Ramasami, Novel triazine-functionalized tetra-imidazolium hexafluorophosphate salt: Synthesis, crystal structure and DFT study, J. Mol. Struct. 1198 (2019) 126902, https://doi.org/10.1016/j.molstruc.2019.126902.

[15] C. Yu, R. Chen, J.J. Li, J.J. Li, M. Drahansky, M.. Paridah, A. Moradbak, A.. Mohamed, H. abdulwahab taiwo Owolabi, FolaLi, M. Asniza, S.H.. Abdul Khalid, T. Sharma, N. Dohare, M. Kumari, U.K. Singh, A.B. Khan, M.S. Borse, R. Patel, A. Paez, A. Howe, D. Goldschmidt, C. Corporation, J. Coates, F. Reading, We are IntechOpen , the world ' s leading publisher of Open Access books Built by scientists , for scientists TOP 1 %, Intech. (2012) 13. https://doi.org/10.1016/j.colsurfa.2011.12.014.

[16] K. Sayin, S.E. Kariper, M. Taştan, T.A. Sayin, D. Karakaş, Investigations of structural, spectral, electronic and biological properties of N-heterocyclic carbene Ag(I) and Pd(II) complexes, J. Mol. Struct. 1176 (2019) 478–487, https://doi.org/10.1016/j.molstruc.2018.08.103.

[17] Amy M. Zimmermann-Klemd, Jakob K. Reinhardt, Thanasan Nilsu, Anna Morath, Chiara M. Falanga, Wolfgang W. Schamel, Roman Huber, Matthias Hamburger, Carsten Gründemann, Fitoterapia Boswellia carteri extract and 3-O -acetyl-alpha-boswellic acid suppress T cell function, Fitoterapia. 146 (2020) 104694, https://doi.org/10.1016/j.fitote.2020.104694.

[18] J.Q. Yu, Y.L. Geng, D.J. Wang, H.W. Zhao, L. Guo, X. Wang, Terpenes from the gum resin of Boswellia carterii and their NO inhibitory activies, Phytochem. Lett. 28 (2018) 59–63, https://doi.org/10.1016/j.phytol.2018.09.010.

[19] Yan-gai Wang, Jin Ren, Jie Ma, Jian-bo Yang, Tengfei Ji, Ai-guo Wang, Bioactive cembrane-type diterpenoids from the gum-resin of Boswellia carterii, Fitoterapia. 137 (2019) 104263, https://doi.org/10.1016/j.fitote.2019.104263.

[20] H.M. Berman, The Protein Data Bank / Biopython, Presentation. 28 (2000) 235–242, https://doi.org/10.1093/nar/28.1.235.

[21] D.R. Koes, M.P. Baumgartner, C.J. Camacho, Lessons learned in empirical scoring with smina from the CSAR 2011 benchmarking exercise, J. Chem. Inf. Model. 53 (2013) (2011) 1893–1904, https://doi.org/10.1021/ci300604z.

[22] Hongjian Li, Kwong-Sak Leung, Pedro J. Ballester, Man-Hon Wong, Julio Vera, Istar: A web platform for large-scale protein-ligand docking, PLoS One. 9 (1) (2014) e85678, https://doi.org/10.1371/journal.pone.0085678.

[23] A. Allouche, Software News and Updates Gabedit — A Graphical User Interface for Computational Chemistry Softwares, J. Comput. Chem. 32 (2012) 174–182, https://doi.org/10.1002/jcc.

[24] W.L. DeLano, Pymol: An open-source molecular graphics tool, CCP4 Newsl, Protein Crystallogr. 40 (2002) 82–92.

[25] and D.J.F. Gaussian 16, Revision C.01, M. J. Frisch, G. W. Trucks, H. B. Schlegel, G. E. Scuseria, M. A. Robb, J. R. Cheeseman, G. Scalmani, V. Barone, G. A. Petersson, H. Nakatsuji, X. Li, M. Caricato, A. V. Marenich, J. Bloino, B. G. Janesko, R. Gomperts, B. Mennu, No TitleGaussian, Inc, Wallingford CT. (2016).

[26] Axel D. Becke, No TitleDensity-functional thermochemistry. III. The role of exact exchange, J. Chem. Phys. 98 (7) (1993) 5648–5652.

[27] Chengteh Lee, Weitao Yang, Robert G. Parr, Development of the Colle-Salvetti correlation-energy formula into a functional of the electron density, Phys. Rev. B. 37 (2) (1988) 785–789.

[28] Æ. Frisch, R.E. Plata, D.A. Singleton, Gaussian 09W Reference, J. Am. Chem. Soc. 137 (2009) 3811–3826, https://doi.org/10.1021/ja5111392.

[29] E.A. Hussein, I.M. Shaheed, R.S. Hatam, M.M. Kadhim, D.T. Al-kadhum, Adsorption, Thermodynamic and DFT Studies of Removal RS Dye on the Iraq Clay from Aqueous, Solutions 11 (2020) 495–502, https://doi.org/10.5530/srp.2020.3.63.

[30] Awadhesh Kumar Singh, Akriti Singh, Altamash Shaikh, Ritu Singh, Anoop Misra, Chloroquine and hydroxychloroquine in the treatment of COVID-19 with or without diabetes: A systematic search and a narrative review with a special reference to India and other developing countries, Diabetes Metab. Syndr. Clin. Res. Rev. 14 (3) (2020) 241–246, https://doi.org/10.1016/j.dsx.2020.03.011.

[31] M. Namazian, S. Halvani, Calculations of p K a values of carboxylic acids in aqueous solution using density functional theory, 38 (2006) 1495–1502. https://doi.org/10.1016/j.jct.2006.05.002.

[32] A. Malijevsk, C. Technology, Physical Chemistry in Brief (2005).

[33] D.C. Warhurst, J.C.P. Steele, I.S. Adagu, J.C. Craig, C. Cullander, Hydroxychloroquine is much less active than chloroquine against chloroquine-resistant Plasmodium falciparum, in agreement with its physicochemical properties, J. Antimicrob. Chemother. 52 (2003) 188–193, https://doi.org/10.1093/jac/dkg319.

[34] C. Skarke, K. Kuczka, L. Tausch, O. Werz, T. Rossmanith, J.S. Barrett, S. Harder, W. Holtmeier, J.A. Schwarz, Increased bioavailability of 11-keto-β-boswellic acid following single oral dose frankincense extract administration after a standardized meal in healthy male volunteers: Modeling and simulation considerations for evaluating drug exposures, J. Clin. Pharmacol. 52 (2012) 1592–1600, https://doi.org/10.1177/0091270011422811.

[35] Tarun Sharma, Snehasis Jana, Investigation of Molecular Properties that Influence the Permeability and Oral Bioavailability of Major β-Boswellic Acids, Eur. J. Drug Metab. Pharmacokinet. 45 (2) (2020) 243–255, https://doi.org/10.1007/s13318-019-00599-z.

[36] E. Eroglu, S. Palaz, O. Oltulu, H. Turkmen, C. Ozaydin, Comparative QSTR study using semi-empirical and first principle methods based descriptors for acute toxicity of diverse organic compounds to the fathead minnow, Int. J. Mol. Sci. 8 (2007) 1265–1283, https://doi.org/10.3390/ijms8121265.